Kinetics and mechanism of the photodecomposition of xenon tetroxide

N. N. Aleinikov, G. K. Vasil'ev, S. A. Kashtanov, E. F. Makarov, and Yu. A. Chernyshev*

Institute of Chemical Physics in Chernogolovka, Russian Academy of Sciences, 142432 Chernogolovka, Moscow Region, Russian Federation. Fax: +7 (096) 515 3588

The of photochemical decomposition of XeO_4 under the action of UV-radiation in the wavelength range of 200—300 nm was investigated. The quantum yield of the formation of oxygen atoms upon XeO_4 photodissociation was measured ($\Phi = 3.6 \pm 0.4$). The results obtained point to the predominant role of the $XeO_4 + h\nu \rightarrow 4O + Xe$ photodissociation channel of XeO_4. The value of the rate constant of the reaction $XeO_4 + O \rightarrow O_2 + XeO_3$ was estimated ($<4.5 \cdot 10^{-16}$ cm^2 s^{-1}).

Key words: xenon tetroxide; photolysis; reaction mechanism.

Along with ozone, xenon tetroxide is known as one of the strongest oxidants. The gas phase chemistry of ozone has been much investigated in recent years — hundreds of papers have dealt only with ozone photolysis. At the same time, there have been no investigations of the gas phase reactions of XeO_4 as far as we know, though they are of considerable interest.

In the present work, the photochemical processes proceeding *via* UV-irradiation of XeO_4 have been studied.

Experimental

The experiments were carried out on the installation shown in Fig. 1. The installation is a quartz tubular reactor (with a diameter of 4.5 cm and a length of 5 cm) equipped with flat windows at the faces for input and output of the probing radiation as well as a flat lateral window for input of radiation from the photolysis lamp. A homogeneous parallel beam shaped by a CaF_2 lens was incident on the lateral window filling nearly the whole reactor volume. The reactor was filled with xenon tetroxide and diluent gases. A deuterium arc lamp with a continuous emission spectrum in the region of 195—300 nm was used as the source of UV-radiation for performing the photolysis. The dynamics of the photochemical decomposition of XeO_4 was traced by changes in the time dependence of the intensity ($I(t)$) of the probing UV-radiation transmitted through the reactor. A low pressure mercury lamp ($\lambda = 253.6$ nm) of much weaker intensity than that of the photolysis lamp was used as the source of probing radiation. In some experiments the probe was carried out at 227 nm. In those cases the deuterium lamp was used simultaneously as both the photolysis and probing source.

In the region of 195—300 nm, xenon tetroxide has a continuous Gaussian absorption spectrum with a half-width of ~400 nm and a maximum at 241 nm. The XeO_4 absorption cross-sections measured at 253.6 and 227 nm are equal to $1.3 \cdot 10^{-17}$ and $1.2 \cdot 10^{-17}$ cm^2, respectively. The concentration of XeO_4 when evaluating the absorption cross-sections was determined iodometrically.[1]

Xenon tetroxide freshly obtained before each experiment by the reaction between powdery sodium perxenate and concentrated sulphuric acid

$$Na_4XeO_6 + 2H_2SO_4 \rightarrow 2Na_2SO_4 + XeO_4 + 2H_2O,$$

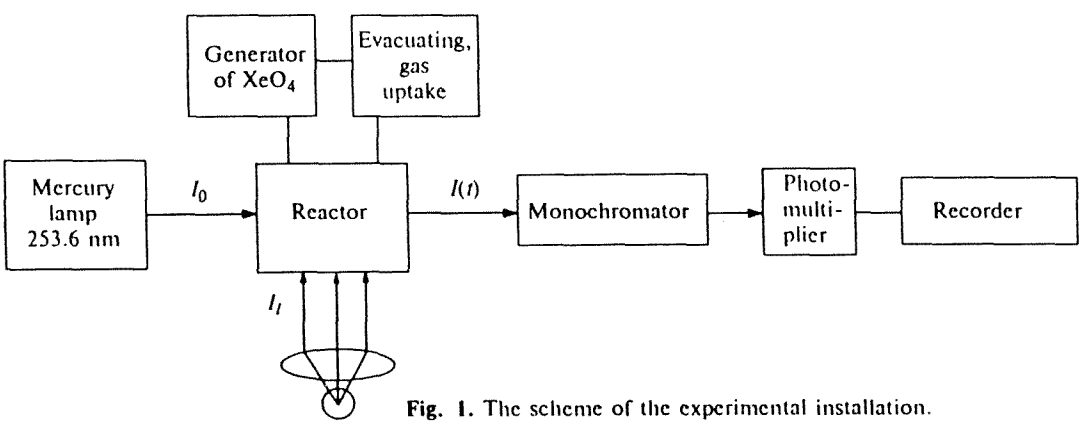

Fig. 1. The scheme of the experimental installation.

Translated from *Izvestiya Akademii Nauk. Seriya Khimicheskaya*, No. 6, pp. 1413—1418, June, 1996.

1066-5285/96/4506-1344 $15.00

was fed to the reactor. The XeO_4 pressure was varied in the range from 0.1 to 0.7 Torr. The use of higher pressure is undesirable because of the considerable inhomogenuity of the UV-radiation in the transverse direction of the reactor due to asbsorption. The yield of XeO_4 in the generator was ~70 %. Oxygen was also among the gaseous products, most likely due to partial decomposition of XeO_4 because of heat liberation in the reaction proceeding mainly in the superficial Na_2XeO_6 layer. Oxygen (O_2), He, Xe, and CO_2 were used as diluent gases.

Results and Discussion

The choice of the model for the photochemical decomposition of XeO_4. In order to determine and interpret the optimum experimental conditions one needs to choose and analyze a model for XeO_4 photolysis that includes the initial step, the photodissociation of XeO_4, and subsequent secondary chemical reactions.

The main characteristics of the photodissociation reaction are the quantum yield and the energetic state of the products formed. There are 4 possible channels of the photodissociation:

$$XeO_4 + h\nu \rightarrow XeO_3 + O, \quad (1a)$$

$$XeO_4 + h\nu \rightarrow Xe + O_2 + 2O, \quad (1b)$$

$$XeO_4 + h\nu \rightarrow Xe + 4O, \quad (1c)$$

$$XeO_4 + h\nu \rightarrow Xe + 2O_2. \quad (1d)$$

Oxygen atoms and molecules forming in the course of decomposition may be in electron-excited states. The generalized equation of photodecomposition (reactions 1a—d) can be written as

$$XeO_4 + h\nu \rightarrow \Phi_1 \cdot O(^3P) + \Phi_2 \cdot O(^1D) + \Phi_3 \cdot O_2(^1\Delta) + \Phi_4 \cdot O_2(^1\Sigma) + \ldots, \quad (1)$$

where Φ_1, Φ_2, Φ_3, Φ_4 are the quantum yields of the formation of $O(^3P)$, $O(^1D)$, $O_2(^1\Delta)$, and $O_2(^1\Sigma)$. The total $\Phi = \Phi_1 + \Phi_2$ quantum yield of the formation of O atoms may vary from 0 to 4.

The most important secondary processes are presented in Scheme 1.

Scheme 1

$$O + O_2 + M \rightarrow O_3 + M, \quad (2)$$
$k_2(M = O_2) = 6.8 \cdot 10^{-34}$ cm^6 s^{-1} (see Ref. 2)

$$O + XeO_4 \rightarrow O_2 + XeO_3 \quad (3)$$

$$O + O_3 \rightarrow 2O_2, \quad (4)$$
$k_4 = 8 \cdot 10^{-15}$ cm^3 s^{-1} (see Ref. 3)

$$O + \text{wall} \rightarrow 1/2O_2 \quad (5)$$

$$O_3 + h\nu \rightarrow O_2(^1\Delta) + O(^1D), \quad (6)$$
$\sigma(253.6\ \text{nm}) = 1.14 \cdot 10^{-17}$ cm^2 (see Ref. 4)
$\sigma(227\ \text{nm}) = 0.34 \cdot 10^{-17}$ cm^2 (see Ref. 4)

$$O(^1D) + XeO_4 \rightarrow XeO_3 + 2O \quad (7)$$

$$O(^1D) + O_3 \rightarrow O_2 + 2O, \quad (8)$$
$k_8 = 2.4 \cdot 10^{-10}$ cm^3 s^{-1} (see Ref. 5)

$$O(^1D) + O_2 \rightarrow O + O_2(^1\Sigma), \quad (9)$$
$k_9 = 4.2 \cdot 10^{-11}$ cm^3 s^{-1} (see Ref. 5)

$$O(^1D) + M \rightarrow O + M, \quad (10)$$
$k_{10}(M = He) = 3 \cdot 10^{-13}$ cm^3 s^{-1} (see Ref. 6)
$k_{10}(M = Xe) = 5 \cdot 10^{-11}$ cm^3 s^{-1} (see Ref. 6)

$$O_2(^1\Delta) + XeO_4 \rightarrow O_2 + XeO_3 + O \quad (11)$$

$$O_2(^1\Delta) + O_3 \rightarrow 2O_2 + O, \quad (12)$$
$k_{12} = 4.4 \cdot 10^{-15}$ cm^3 s^{-1} (see Ref. 7)

$$O_2(^1\Delta) + M \rightarrow O_2 + M, \quad (13)$$
$k_{13}(M = O_2) = 1.6 \cdot 10^{-18}$ cm^3 s^{-1} (see Ref. 8)
$k_{13}(M = He) = 8 \cdot 10^{-21}$ cm^3 s^{-1} (see Ref. 7)

$$O_2(^1\Delta) + \text{wall} \rightarrow O_2 \quad (14)$$

$$O_2(^1\Sigma) + XeO_4 \rightarrow O_2 + XeO_3 + O \quad (15)$$

$$O_2(^1\Sigma) + O_3 \rightarrow 2O_2 + O, \quad (16)$$
$k_{16} = 1.96 \cdot 10^{-11}$ cm^3 s^{-1} (see Ref. 6)

$$O_2(^1\Sigma) + M \rightarrow O_2(^1\Delta) + M, \quad (17)$$
$k_{17}(M = O_2) = 4 \cdot 10^{-17}$ cm^3 s^{-1} (see Ref. 9)
$k_{17}(M = He) = 2.5 \cdot 10^{-16}$ cm^3 s^{-1} (see Ref. 6)

The particles in the ground state are denoted by O and O_2 in Scheme 1. The values of the corresponding rate constants known from the literature are also listed in Scheme 1 (see also Ref. 10). Secondary processes with participation of XeO_3 molecules are not included in Scheme 1, since according to thermochemical data, the energy of the cleavage of the first Xe—O bond in the XeO_3 molecule is considerably higher and, hence, its reactivity is lower than in the XeO_4 molecule. Neither is the photodissociation of XeO_3 molecules included in Scheme 1, since the accumulation of the latter in appreciable amounts is ruled out.

This is associated with the fact that XeO_3 is a solid (with a low vapor pressure) at room temperature, and therefore, its molecules will either be adsorbed by the reactor walls or "stick together" in collisions with each other to yield microparticles.

Applying the quasi-stationary concentrations method to O, $O(^1D)$, $O_2(^1\Delta)$, and $O_2(^1\Sigma)$ particles, we obtain:

$$-\frac{d[XeO_4]}{dt} = \{1 + \gamma_1\Phi_1 + [\beta_2(\rho_2 + \gamma_1) + \beta_3(1 - \beta_2)(\rho_3 + \gamma_1)]\Phi_4\}k_1[XeO_4] + \{\rho_1\beta_1 + \beta_4[\rho_2\beta_2 + \rho_3\beta_3(1 - \beta_2)] + \gamma_1[1 + \beta_1 + \beta_4(\beta_2 + \beta_3(1 - \beta_2))]\}\{\Phi_2k_1[XeO_4] + k_6[O_3]\} + \beta_3(\rho_3 + \gamma_1)\{\Phi_3k_1[XeO_4] + k_6[O_3]\}; \quad (18)$$

$$-\frac{d[O_3]}{dt} = k_6[O_3] + \{[(1-\rho_2)\beta_2 + (1-\rho_3)(1-\beta_2)\beta_3]\Phi_4 + (\gamma_2-\gamma_3)[\Phi_1 + (\beta_2 + \beta_3(1-\beta_2))\Phi_4]\}k_1[XeO_4] + \{(1-\rho_1)\beta_1 + \beta_4[(1-\rho_2)\beta_2 + (1-\rho_3)(1-\beta_2)\beta_3] + (\gamma_2-\gamma_3)[1 + \beta_1 + \beta_4(\beta_2 + \beta_3(1-\beta_2))]\} \times \{\Phi_2 k_1[XeO_4] + k_6[O_3]\} + \beta_3(1-\rho_3+\gamma_2-\gamma_3)\{\Phi_3 k_1[XeO_4] + k_6[O_3]\}, \quad (19)$$

where $k_1 = \int\sigma_1(\nu)I_1(\nu)d\nu$, $k_6 = \int\sigma_2(\nu)I_1(\nu)d\nu$ are the specific rates of photodissociation of XeO_4 and O_3 molecules in processes (1) and (6); $\sigma_1(\nu)$, $\sigma_2(\nu)$ are the absorption cross-sections of XeO_4 and O_3 at frequency ν; $I_1(\nu)$ is the irradiation intensity of the photolysis lamp.

$$\beta_1 = \frac{k_7[XeO_4] + k_8[O_3]}{k_7[XeO_4] + k_8[O_3] + k_9[O_2] + k_{10}[M]};$$

$$\beta_2 = \frac{k_{15}[XeO_4] + k_{16}[O_3]}{k_{15}[XeO_4] + k_{16}[O_3] + k_{17}[M]};$$

$$\beta_3 = \frac{k_{11}[XeO_4] + k_{12}[O_3]}{k_{11}[XeO_4] + k_{12}[O_3] + k_{13}[M] + k_{14}};$$

$$\beta_4 = \frac{(1-\beta_1)k_9[O_2]}{k_9[O_2] + k_{10}[M]};$$

$$\rho_1 = \frac{k_7[XeO_4]}{k_7[XeO_4] + k_8[O_3]}; \quad \rho_2 = \frac{k_{15}[XeO_4]}{k_{15}[XeO_4] + k_{16}[O_3]};$$

$$\rho_3 = \frac{k_{11}[XeO_4]}{k_{11}[XeO_4] + k_{12}[O_3]};$$

$$\gamma_1 = \frac{k_3[XeO_4]}{k_2[O_2][M] + k_3[XeO_4] + k_4[O_3] + k_5};$$

$$\gamma_2 = \frac{k_4[O_3]}{k_2[O_2][M] + k_3[XeO_4] + k_4[O_3] + k_5};$$

$$\gamma_3 = \frac{k_2[O_2][M]}{k_2[O_2][M] + k_3[XeO_4] + k_4[O_3] + k_5}.$$

Here $0 \le \beta_i \le 1$; $0 \le \rho_i \le 1$; $0 \le \gamma_i \le 1$. For the reaction scheme given above, Eqs. (18) and (19) describe all possible cases. A further problem consists in choosing experimental conditions for which the equations can be simplified.

Photolysis of XeO_4 in the presence of O_2. Experiments on the photolysis of XeO_4 in the presence of O_2 were carried out with the aim of determining the quantum yields of the formation of oxygen atoms (Φ); reaction (2) was used in order to turn the oxygen atoms into ozone molecules that could be detected by spectroscopic techniques. If xenon tetroxide is highly diluted with oxygen, reactions (2) and (9) must suppress reactions (3)—(5) and (7) and (8), respectively. If $k_2[O_2][M] \gg k_3[XeO_4] + k_4[O_3] + k_5$; $k_9[O_2] \gg k_7[XeO_4] + k_8[O_3]$, then $\beta_1 = 0$; $\beta_4 = 1$; $\gamma_1 = 0$; $\gamma_2 = 0$; $\gamma_3 = 1$. Because of the large k_{16}/k_{17} ratio of the rate constants already at an ozone concentration of $[O_3] > 10^{14}$ cm^{-3}, corresponding to less than 1 % XeO_4 conversion, we get $k_{16}[O_3] \gg k_{17}[M]$, *i.e.* $\beta_2 = 1$. One can simplify Eqs. (18) and (19):

$$-\frac{d[XeO_4]}{dt} = [1 + \rho_2(\Phi_2 + \Phi_4) + \rho_3\beta_3\Phi_3]k_1[XeO_4] + (\rho_2 + \rho_3\beta_3)k_6[O_3]; \quad (20)$$

$$\frac{d[O_3]}{dt} = [\Phi + \rho_2(\Phi_2 + \Phi_4) + \rho_3\beta_3\Phi_3]k_1[XeO_4] + (\rho_2 + \rho_3\beta_3)k_6[O_3]. \quad (21)$$

The initial conditions are: at $t = 0$ $[XeO_4] = [XeO_4]_{ini}$; $[O_3] = 0$.

The system of equations (20) and (21) describes the loss of XeO_4 and the formation of O_3 after photolysis of the gas mixture, respectively. After time $t = (3-5)/k_1$ ($1/k_1$ is the characteristic time of XeO_4 photodissociation), the process is completed, and the final ozone concentration $[O_3]_{fin}$ is achieved.

Denoting

$$A_1 = \int k_1[XeO_4]dt,$$

$$A_2 = \int\{[\rho_2(\Phi_2 + \Phi_4) + \rho_3\beta_3\Phi_3]k_1[XeO_4] + (\rho_2 + \rho_3\beta_3)k_6[O_3]\}dt$$

and having integrated the system (20)—(21) from 0 to t, we get

$$[XeO_4]_{ini} = A_1 + A_2; \quad [O_3]_{fin} = \Phi A_1 + A_2.$$

Hence,

$$[O_3]_{fin}/[XeO_4]_{ini} = (\Phi A_1 + A_2)/(A_1 + A_2)$$

and

$$\Phi = [O_3]_{fin}/[XeO_4]_{ini} + ([O_3]_{fin}/[XeO_4]_{ini} - 1)A_2/A_1.$$

Taking into account that

$$[XeO_4]_{ini} = -(1/(\sigma_1 L)) \cdot \ln(I_{ini}/I_0),$$
$$[O_3]_{fin} = -(1/(\sigma_2 L)) \cdot \ln(I_{fin}/I_0),$$

under the condition $[O_3]_{fin}/[XeO_4]_{ini} > 1$ we eventually get:

$$\Phi = \frac{[O_3]_{fin}}{[XeO_4]_{ini}} = \frac{\sigma_1}{\sigma_2}\frac{\ln(I_{fin}/I_0)}{\ln(I_{ini}/I_0)}. \quad (22)$$

Here I_0 is the intensity of probing radiation in front of the reactor; I_{ini}, I_{fin} is the intensity of probing radiation transmitted through the reactor before the beginning and at the end of photolysis, respectively; L is the reactor length; σ_1 and σ_2 are the absorption cross-sections of XeO_4 and O_3 at the wavelength of probing radiation, respectively. For any moment of time $I = I_0\exp[-(\sigma_1[XeO_4] + \sigma_2[O_3])L]$, so using Eqs. (20) and (21) we obtain:

$$-\frac{1}{I}\frac{dI}{dt} = \sigma_1 L\left\{\left|\frac{\sigma_2}{\sigma_1}\Phi - 1 - \frac{\Delta\sigma}{\sigma_1}(\rho_2(\Phi_2 + \Phi_4) + (\rho_3\beta_3\Phi_3)\right]k_1[XeO_4] - \frac{\Delta\sigma}{\sigma_1}(\rho_2 + \rho_3\beta_3)k_6[O_3]\right\},$$
$$\Delta\sigma = \sigma_1 - \sigma_2.$$

Since $\sigma_1 \approx \sigma_2$ for probing radiation at the wavelength of 253.6 nm, without making an appreciable error, one

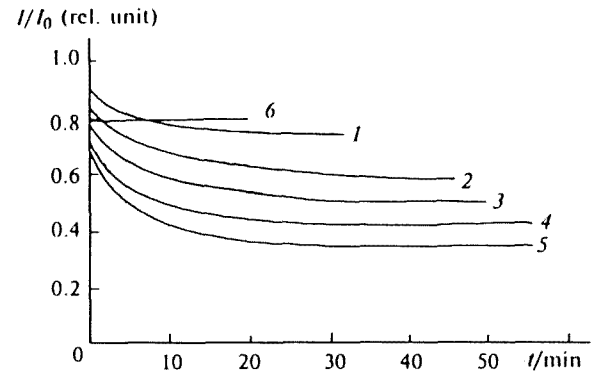

Fig. 2. Change in the intensity of probing radiation in the course of the photochemical decomposition of XeO_4 in mixtures with O_2 (initial pressure of XeO_4 (p_1) and O_2 pressure (p_2), Torr): at λ = 253.6 nm: *1*, p_1 = 0.05, p_2 = 350; *2*, p_1 = 0.085, p_2 = 525; *3*, p_1 = 0.12, p_2 = 480; *4*, p_1 = 0.15, p_2 = 360; *5*, p_1 = 0.18, p_2 = 360; at λ = 227 nm: *6*, p_1 = 0.11, p_2 = 375.

can disregard the addends containing the $\Delta\sigma/\sigma_1$ multiplier:

$$-\frac{1}{I}\frac{dI}{dt} = \sigma_1 L(\Phi - 1)k_1[XeO_4]. \qquad (23)$$

This relationship allows one to obtain the value of the $k_1(\Phi - 1)$ parameter and, hence, the characteristic time $\tau_1 = 1/k_1$ (or the specific rate k_1) of XeO_4 photodissociation from the derivative on the initial part of the transmission curve $I(t)$.

In experiments on the photochemical decomposition of XeO_4 in the presence of O_2, the initial pressure of xenon tetroxide was varied in the range from 0.1 to 0.45 Torr, and the pressure of O_2 was varied from 200 to 600 Torr. Thirty experiments were carried out. Typical dependences of the intensity of probing radiation transmitted through the reactor during the photolysis are shown in Fig. 2. In most experiments, the probing was carried out at a wavelength of 253.6 nm. In this case conversion of XeO_4 was accompanied by an increase in absorption (curves *1*—*5*). The photolysis was performed for 1 h until a constant intensity of transmitted light was reached. The intensity of the transmitted probing radiation at 227 nm remained constant (with an accuracy of ±2 %) in the course of the photochemical decomposition of XeO_4 (see curve *6* in Fig. 2). The processing of probe data (λ = 253.6 nm) gave the mean value of the $[O_3]_{fin}/[XeO_4]_{ini}$ ratio equal to 3.2, *i.e.* in accordance with Eq. (22) $\Phi \geq 3.2$. The relationship $I_{fin} \approx I_{ini}$ is valid if the probing is carried out at 227 nm; hence, $[O_3]_{fin}/[XeO_4]_{ini} = \sigma_1/\sigma_2 = 3.5$, and $\Phi \geq 3.5$. Since Φ cannot exceed 4, $3.2 \leq \Phi \leq 4$, and $\Phi = 3.6 \pm 0.4$. The Φ value found allows one to draw the conclusion that the predominant channel of photodissociation of the XeO_4 molecule is channel (1c) with the formation of four oxygen atoms. The problem of the decomposition dynamics is still an open question, since it is not clear whether the decomposition follows a single-step mechanism with simultaneous cleavage of all bonds or is a multi-step mechanism with the formation of short-lived intermediate fragments (XeO_2, XeO).

The data processing for the initial parts of the $I(t)$ curves according to Eq. (23) allowed one to determine the mean value of the $k_1(\Phi - 1)$ parameter to be equal to 0.217 min^{-1}. Using the value of Φ = 3.6, the specific rate of photodissociation of the XeO_4 molecules under the experimental conditions was obtained: k_1 = 0.0835 min^{-1}.

Photolysis of XeO_4 in the presence of He, Xe, and CO_2. The experiments on the photolysis of XeO_4 in mixtures with O_2 were carried out such that reaction (2) was predominant in the abstraction of O atoms. This allowed us to determine the quantum yield of the formation of O atoms during the photodissociation of the XeO_4 molecule as well as the characteristic rate of photodissociation of XeO_4 molecules under the action of light with wavelengths from 200 to 300 nm. Changing the conditions of photochemical decomposition, one can obtain additional information on other processes involved in its mechanism. Thus, the replacement of O_2 by other diluent gases allows one to create conditions in which the rate of reaction (3) could be compared with the known rate of reaction (2), and, hence, the rate constant k_3 could be determined.

Helium as well as Xe and CO_2 were used in experiments as diluent gases; their pressure was varied from 0 to 760 Torr. The probe was carried out at 253.6 nm. About 80 experiments were carried out. The transmission curves of the probing radiation obtained during irradiation of the mixtures of XeO_4 with CO_2 by a deuterium lamp are presented in Fig. 3. It can be seen that a decrease (curves *1*, *2*) or an increase (curves *4*, *5*)

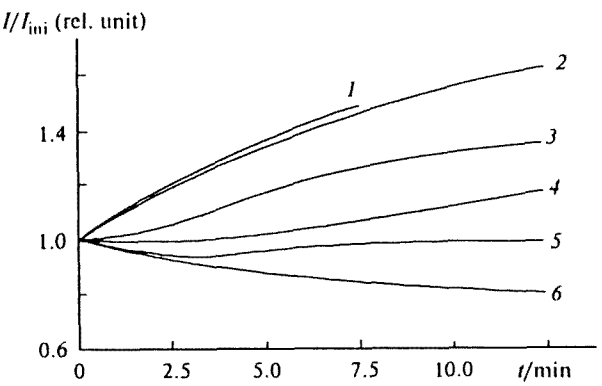

Fig. 3. Change in the intensity of probing radiation in the course of the photochemical decomposition of XeO_4 in mixtures with CO_2 (initial pressure of XeO_4 (p_1), O_2 pressure (p_2), CO_2 pressure (p_3), Torr): at λ = 253 nm and p_1 = 0.47: *1*, p_3 = 7.5; *2*, p_3 = 30; *3*, p_3 = 75; *4*, p_3 = 225; *5*, p_3 = 450; at p_1 = 0.1: *6*, p_3 = 600, p_2 = 0.75.

in absorption at the initial stage of the photolysis as well as a delay between the moment the deuterium lamp is switched on and the beginning of the absorption drop is observed depending on the CO_2 pressure (curve *3*). Addition of O_2 results in an increase in the absorption (curve *6*).

Analogous dependences were also observed when the photolysis of mixtures of XeO_4 with He and Xe was performed. In the case of He, the XeO_4 consumption rate (w) was determined from the formula

$$w = \frac{1}{\ln(I / I_0)} \frac{d \ln(I / I_0)}{dt}$$

from the initial part of the curve of the transmission of the probing radiation (the degree of XeO_4 conversion ≤30 %) where w is nearly constant. At low He pressure, w coincides with the specific rate of xenon tetroxide consumption $(1/[XeO_4]) \cdot (d[XeO_4]/dt)$, since in this case ozone is produced in negligible amounts. As can be seen from Fig. 4, the XeO_4 consumption rate decreases appreciably after adding small amounts of He. Similar results were obtained in experiments with Xe and CO_2. In the absence of diluents, the specific rate of XeO_4 decomposition does not depend on its initial pressure (in the investigated range from 0.1 to 0.6 Torr) and is equal to $w = 0.3$ min^{-1}.

One can assume that the character of the dependences shown in Fig. 3 is determined by competition of the processes of the formation of O_3 from doped oxygen (formed in the course of XeO_4 synthesis, see above) and the loss of XeO_4 and O_3. Assuming without making an appreciable error that $\sigma_1 = \sigma_2 = s$ at $\lambda = 253.6$ nm and using Eqs. (18) and (19), we obtain

$$\frac{1}{I} \frac{dI}{dt} = -\sigma L \frac{d([XeO_4] + [O_3])}{dt} = a - b\gamma,$$

where a and b are the positive parameters ($a/b < 1$) and

$$\gamma = \gamma_3 - \gamma_1 - \gamma_2 = \frac{k_2[O_2][M] - k_3[XeO_4] - k_4[O_3]}{k_2[O_2][M] + k_3[XeO_4] + k_4[O_3] + k_5}.$$

"Brightening" ($dI/dt > 0$) is observed at $g < a/b$, while "darkening" ($dI/dt < 0$) occurs at $g > a/b$. In the extreme cases, $k_2[O_2][M] \gg k_3[XeO_4] + k_4[O_3] + k_5$ (discussed in the preceding section) and $k_2[O_2][M] < k_3[XeO_4] + k_4[O_3]$, "darkening" at $g = 1 > a/b$ and "brightening" at $g < 0 < a/b$ are observed, respectively. Therefore, in successive experiments with increasing $[O_2][M]$ product, a smooth change from "brightening" to "darkening" of a mixture will take place. When a "delay" arises, $\gamma_3 > \gamma_1 + \gamma_2$, and consequently $k_3 < k_2[O_2][M]/[XeO_4]$.

In mixtures with CO_2 the delay was detected at a CO_2 pressure of 75 Torr (see Fig. 3, curve *3*), while in mixtures with He it occured at 115 Torr. Assuming that the concentration of the doped oxygen has its most probable value $0.29[XeO_4]_{ini}$ (which corresponds to a 70 % yield of XeO_4 in the generator and presuming Xe and O_2 to be products of the partial decomposition of XeO_4), we obtain $k_3 < 10^{-15}$ cm^3 s^{-1} and $k_3 < 4.5 \cdot 10^{-16}$ cm^3 s^{-1} for experiments with CO_2 and He, respectively. In our estimate we assumed $k_2(M = CO_2)$ be equal to $1.5 \cdot 10^{-33}$ and $k_2(M = He)$ to be $4 \cdot 10^{-34}$ cm^6 s^{-1}.[11]

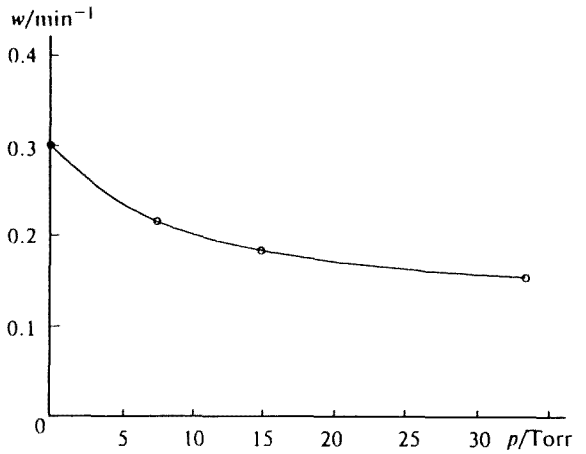

Fig. 4. Dependence of the specific rate of photodecomposition of XeO_4 on He pressure (p).

The most probable reason for the decrease in the XeO_4 consumption rate as He pressure increases (see Fig. 4) is the increasing role of the trimolecular extinction of O atoms in process (2). At not too high pressures, $\beta_1 \simeq 1$, $[O_3] \ll [XeO_4]$. Then for the specific rates of the loss of both non-diluted XeO_4 (w_1) and the loss of that diluted with helium (w) we obtain from Eqs. (18) and (19):

$$w_1 = k_1 \left\{ 1 + \Delta\Phi + (\Phi + \Delta\Phi) \frac{k_3[XeO_4]}{k_3[XeO_4] + k_5} \right\}, \quad (24)$$

$$w = k_1 \{ 1 + \Delta\Phi + (\Phi + \Delta\Phi) \frac{k_3[XeO_4] + k_4[O_3] - k_2[O_2][M]}{k_3[XeO_4] + k_4[O_3] + k_2[O_2][M] + k_5} \}, \quad (25)$$

where $\Delta\Phi = \Phi_2 + \beta_3\Phi_3 + (\beta_2 + \beta_3(1 - \beta_2))\Phi_4$. It follows from (24) and (25) that:

$$\frac{w_1}{w} < \left\{ 1 + \frac{k_2[O_2][M]}{k_3[XeO_4]} \right\} \cdot \left\{ 1 - \frac{k_2[O_2][M]}{k_3[XeO_4]} \right\}^{-1}. \quad (26)$$

From expression (26) we determine $k_3[XeO_4] < \frac{w_1/w + 1}{w_1/w - 1} k_2[O_2][M]$. Using data from Fig. 4 we calculate $k_3 < 2 \cdot 10^{-16}$ cm^3 s^{-1}, which does not contradict the previous estimate. In accordance with formula (24) the independence of the XeO_4 photodissociation rate from the $[XeO_4]_{ini}$ concentration is possible if $k_3[XeO_4]_{ini} > k_5$ in the range under study. One can not rule out another explanation for the dependences shown in Figs. 4 and 5, namely, the formation of "hot" atoms

during primary photodissociation. Thus, energy equal to 0.8—2.3 eV is released in the dominant channel (1c) depending on the magnitude of the quantum absorbed by the translational degrees of freedom of the O atoms. If all of the hot atoms formed react with XeO_4 molecules, then w will be independent of the XeO_4 concentration. Hot atoms rapidly lose their energy in collisions with other particles. According to calculations, the energy of O atoms drops by a factor of e after 3, 5, and 7 collisions with He, O_2, and XeO_4, respectively. In other words, after ≈10 collisions the O atom gets thermalized. From this it follows that the effect associated with hot atoms can be observed if their k_3 constant is larger than 10^{-11} cm^3 s^{-1}, otherwise the atoms will be cooled before the reactionary collision.

It follows from formula (24) that if $k_3[XeO_4] \gg k_5$ then $w_1/k_1 \simeq 1 + \Phi + 2\Delta\Phi$, *i.e.* $w_1/k_1 \simeq 4.6 + 2\Delta\Phi$. The experimental value of that ratio coincides with the theoretical one within the limits of experimental errors (if $\Delta\Phi$ is small), *i.e.* $w_1/k_1 = 0.3/0.0835 = 3.6$. Since $\Phi_2 < \Delta\Phi$, one can draw the conclusion that the yield of the formation of electron-excited O atoms at the first stage of photodissociation can not be large. This conclusion is reasonable if one keeps in mind the fact that the principal channel of decomposition of the XeO_4 molecule is channel (1c) which produces O atoms in ground state. In fact, decomposition through (1c) with the formation of one $O(^1D)$ atom is spin-forbidden, and decomposition with the formation of two $O(^1D)$ atoms is energy-forbidden. The problem of the quantum yield (Φ_2) of formation of $O(^1D)$ can also be solved by comparison of experimental data on XeO_4 decomposition in the mixtures with He and Xe. Xenon quenches $O(^1D)$ atoms with an efficiency which is 170 times higher than that of helium. Therefore, in the case of the formation of $O(^1D)$ atoms in appreciable amounts, the replacement of He by Xe must result in a decrease in the XeO_4 consumption rate. However, this has not been observed in the experiments; so this fact again confirms the conclusion that the quantum yield Φ_2 is small.

Thus, all experimental data on the photochemical decomposition of XeO_4 are described by a non-chain mechanism including processes (1)—(17). The predominant channel of XeO_4 photodissociation is (1c), which yields O atoms in the ground state. The rate constant of the elementary reaction (3) in which the XeO_4 molecule participates is an order of magnitude or more lower than that of reaction (4), in which the O_3 molecule participates. Since these processes are the reactions of the loss of active centers in corresponding oxidation mechanisms, XeO_4 is a more efficient oxidant than O_3.

References

1. H. Selig, H. H. Claassen, C. L. Chernick, J. G. Malm, and J. L. Huston, *Science*, 1964, **143**, 1322.
2. O. Klais, P. C. Anderson, and M. G. Kurylo, *Intern. J. Chem. Kinet.*, 1980, **12**, 469.
3. D. D. Davis, W. Wong, and J. Lephardt, *Chem. Phys. Lett.*, 1973, **22**, 273.
4. M. Griggs, *J. Chem. Phys.*, 1968, **49**, 857.
5. S. T. Amimoto, A. R. Force, R. G. Gulloty, and J. R. Wiesenfeld, *J. Chem. Phys.*, 1979, **71**, 3640.
6. J. Shi and J. R. Barker, *Intern. J. Chem. Kinet.*, 1990, **22**, 1283.
7. R. J. Collins, D. Husain, and R. J. Donovan, *J. Chem. Soc. Faraday Trans. 2*, 1973, **69**, 145.
8. A. P. Billington and P. Borell, *J. Chem. Soc. Faraday Trans. 2*, 1986, **82**, 963.
9. R. L. Martin, R. B. Kohen, and J. F. Schatz, *Chem. Phys. Lett.*, 1976, **41**, 394.
10. I. I. Morosov and S. M. Temchin, *Khimiya plasmy* [*The Chemistry of Plasma*], под ред. B. M. Smirnov, Energoatomizdat, Moscow, 1990, 39 (in Russian).
11. V. N. Kondrat'ev, *Konstanty skorosti gazofaznykh reaktsii* [*The Rate Constants of Gas Phase Reactions*], Nauka, Moscow, 1970, 78 (in Russian).

Received May 4, 1995